Development of oxide dispersion strengthened 2205 duplex stainless steel composite

Oladayo OLANIRAN[1,2 *], Benjamin Omotayo ADEWUYI[1], James Ajibade OMOTOYINBO[1], Ayodeji Ebenezar AFOLABI[1], Davies FOLORUNSO[1], Adekunle ADEGBOLA[3], Emanuel IGBAFEN[1]

[1] *Chemical and Metallurgy Department, Tshwane University of Technology, Pretoria*
[2] *Metallurgical and Materials Engineering Dept., Federal University of technology, Akure*
[3] *The Polytechnic, Mechanical Engineering Department, Ibadan*
E-mails: oladayolaniran@gmail.com; tayo_adewuyi@yahoo.com;
badetoyinbo@yahoo.com; ayode86@yahoo.com; stdavies@yahoo.com;
kunleade@yahoo.com; igbafene@futa.edu.ng
[*]Corresponding author, phone: +2348035001939

Abstract

Duplex stainless steels have a wide range of engineering applications, mainly in automotive, energy, chemical, mining as well as medical industries. The need for advanced researches to improve on the properties is therefore, very important and urgent. This work aims at developing composites of duplex stainless steel by oxide dispersion strengthening method using hot press sintering technique. Powder of ceramic oxide (partially stabilized Zirconia - PSZ, 3% yttria, mole fraction) were dispersed in 2205 duplex stainless steel powders. The ceramic oxide (PSZ) was added as reinforcement, while chromium (Cr) and Nickel (Ni) were incorporated to maintain the austenitic/ferritic phase balance of the duplex stainless steel. The powders and sintered were characterized in detail using scanning electron microscopy (SEM) and X-ray diffraction (XRD). The microstructural evolution and phase formation during oxide dispersion strengthening of duplex stainless steels composites were investigated. The influences of composition variation of the reinforcements on the microstructural and corrosion behavior of the

composites in simulated mine water were investigated. In this work, it was established that composition has great influence on the structure/properties relationship of the developed composites.

Keywords

Strengthening; Metal matrix composite; Sintering; Corrosion; Composites

Introduction

Powder metallurgy allows composite materials, notably metal – ceramic composites, to be produced by sintering a mixture of powders. It consists in consolidating powder mixture by successive pressing and sintering or hot pressing [1]. The densification of metal – ceramic powder mixture during hot pressing has been largely studied. It has been shown in particular that particle size ratio has a prominent effect on the densification kinetics. The final density plays a major role on the mechanical properties of the sintered composite; it is important to have it as high as possible [2-5]. Experimental work about densification of powder mixtures during sintering have been studied by different researchers. Youngmoo et al. worked on the fabrication of high temperature oxides dispersion strengthened tungsten composition by spark plasma sintering process [6] and Wong et al. also developed Mg/Cu nanocomposites using microwave assisted rapid sintering [7]. Datta and Upadhyaya developed duplex stainless steels from premixes of 316L and 434L powders [8]. However, Olmos et al, in their work, demonstrated that a very small amount of inclusion (typically 3 vol.%) can significantly affect the densification which has been attributed to different phenomena such as inclusion induced stress, heterogeneity and network formation [1].

Nanocrystalline materials have attained great scientific interests in the recent years because these possess superior mechanical, physical and chemical properties compared to conventional coarse – grained materials [2, 5]. Nanostructured solids with dispersion strengthening offered by uniform distribution of nano-intermetallic or nano-ceramic phases are extremely useful for structural applications at ambient or at elevated temperatures. Ceramic oxide dispersion strengthened steel find wide applications in fabricating discs and other critical parts of jet engines, pump bodies and parts, nuclear fuel element spacers etc. Nano – Y_2O_3 (Yttrium Oxide Nanoparticles) dispersed steel possess a combination of body

cantered cubic (BCC) structure with low coefficient of thermal expansion, high thermal conductivity, good creep resistance and high tensile/compressive strength as reported by [4] and [9].

Ceramic reinforcement with zirconia can exist in three forms; cubic, tetragonal and monoclinic. Transformation from the tetragonal to the monoclinic modification is followed by a volume change resulting in catastrophic fracture and hindering the application of pure ZrO_2 composites. Stabilizers such as Y_2O_3, CaO, MgO allows the stabilization down to room temperature [9]. Zirconia stabilized with 3 mol% yttria was selected for its particular mechanical and thermal properties such as high melting point, high hardness, high electrical conductivity, excellent corrosion resistance against molten iron and slag, superb thermal shock resistance. These properties make it an excellent candidate for very high temperature applications as in combustion chambers, thermal protection shields for space vehicles etc. [10, 11].

Mechanical alloying is a useful technique to synthesize novel materials including nanostructured and amorphous products in powder form, consolidation of such powders into a bulk component without deteriorating or destroying the as – milled novel mictrostructural state poses a genuine challenge. Various attempts that have achieved reasonable success in this regard are high pressure sintering, equi – channel angular pressing, laser sintering, pulse plasma sintering and hot isostatic pressing as reported by Karak [4]. However, studies on hot pressing of nano-oxide dispersed mechanically alloyed steel are scarce, which informed the development of oxide dispersion strengthened duplex stainless steel composites and investigate the influence of composition variation on the corrosion behavior of the developed composites. Our aims was to develope composites of duplex stainless steel by oxide dispersion strengthening method using hot press sintering technique.

Materials and method

Sample preparation

Mixture of atomized polycrystalline 2205 supplied be WEARTECH Ltd., South Africa with composition presented in Table 1, partially stabilized Zirconia (PSZ, 3%yttria, mole fraction), chromium and Nickel were used in this study.

Table 1. Chemical composition of as received 2205 DSS

	Cr (%)	Ni (%)	Mo (%)	Si (%)	N (%)	P (%)	C (%)	Mn (%)	S (%)
2205	22.8	5.1	3.3	0.77	0.25	0.014	0.012	0.98	0.006
	Al (%)	Co (%)	Cu (%)	P (%)	Sn (%)	Ti (%)	W (%)	B (%)	Fe (%)
	-	-	-	-	-	-	-	-	Balance

The powders particle sizes as stated by the suppliers are: Duplex stainless steel (2205) –22µm, partially stabilized Zirconia (PZY) is 50nm; chromium and Nickel are -325mesh and 4.5µm respectively. XRD was used to determine the phase present. Different composites were produced by weighing different percentages of the matrix, the reinforcement and the alloying elements as indicated in Table 1 to give X, A1, A2, A3, A4 and A5. These weighed powders were mixed in the TUBULA® mixer for 2 hours, after which the admixed powders were sintered in a hot press; High Temperature, High Pressure (HTHP) at sintering temperature of 1100°C, pressure of 30 MPa and 30 minutes holding time using Argon gas flow to achieve a consolidated bulk cylindrical composite of 18 mm diameter and 2 mm thickness.

Scanning electron microscope (SEM) with a link energy dispersive X-ray spectroscopy (EDS) detector attachment, model JEOL, JSM – 7600F, were used to assess shape of agglomeration of particles and the compositions of the various ODS composite. The phase identification was determined using X-ray diffraction PAN analytical X'pert PRO with Co anode, step size of 2θ (generating settings 30kv, 10mA), while the elemental compositions were identified using the EDS. The densities of the sintered samples were measured using Archimedes principle after weighing in air and water separately using an electronic balance of 0.1mg precision. Morphology, shape and size distribution of the phases in the sintered components were studied using a field emission scanning electron microscopy (FESEM). Relative density was calculated from the sintered density and theoretical density and the latter was deduced from the simple law of mixture; $\rho_t = \rho_1 f_1 + \rho_2 f_2 + \ldots + \rho_n f_n$, where ρi and fi are the theoretical density and the volume fraction of component i.

Results and discussion

The result for characterization of the as received 2205 powder is presented in Figure 1, while the results for the densification of the ceramic oxide reinforced composites is presented

in Table 2 and the SEM micrographs of the sintered samples were also presented in Figure 2.

Density/Porosity

From the densification presented in Table 1, it was evident that the materials were well sintered with good densification. It was also observed that the densification of the sintered sample was increasing with percentage increase in the reinforcement. Sample 1 with 0.5% reinforcement has a densification of 99.74% while sample 5 with 2% $ZrO_2(Y_2O_3)$ has a densification of 99.87%. This was possibly due to good wettability of Zr with Fe which is in agreement with [10, 12]. The effect of Cr and Ni also contributed to the densification obtained. Considering the features of Cr, its hardness and abrasiveness tend to reduce densification [1, 12] but rather, promote pores formation. The presence of Ni as one of the alloying elements, considering it's melting point, acts as a binder and thus try to bind the grains/powder particles of the composite and thereby reduces the porosity. This was influenced by the percentage composition of the Ni to Cr present in the composite. The basic mechanisms include vapor transport and surface, volume and grain boundary diffusion. This vapor transport and surface diffusion mechanisms bonding affect pore rounding but not densification. This was evident in samples 2 and 3 respectively. The presence of Y_2O_3 as a stabilizer in the reinforcement also influences the densification [14, 15].

Table 2. Properties of hot pressed DSS composites

Sample	Density ($g/cm^{3)}$	Theoretical density (g/cm^3)	Relative density (%)	Open porosity (%)	Vickers Hardness Value (Hv0.1)
X	7.72	7.7	99.60	0.4	847.01
A1	7.68	7.73	99.35	0.65	916.13
A2	7.67	7.71	99.48	0.52	845.02
A3	7.69	7.72	99.51	0.40	852.11
A4	7.64	7.69	99.50	0.50	881.02
A5	7.62	7.66	99.53	0.40	835.02

Microstructure

PM steels usually possess residual porosity and heterogeneous microstructure, which arises from inhomogeneous distribution of alloying powders [13-15]. There were observations of pores in the SEM images of the sintered specimens but distributions and sizes differ, which is one of the characteristics of sintered specimen from PM on the basis of their primary particle size and material density [16]. Figure 1 obtained from SEM represent powder particle

shapes, sizes and distribution of as received 2205 powder. The shapes are spherical comprising of smaller and bigger sizes which are evenly distributed within the matrix. The SEM images were analyzed at 500 microns. The characterized 2205 was shown in Figure 1; SEM image and Table 3; the EDS spot analysis. From the EDS analyses, the expected elemental compositions were detected. EDS results show that Fe contents is the largest and appeared as spherical and grey particle, this was clearly seen in spectrum 5. Cr and Ni were also detected though, Ni has low content. Admix were also characterized. Though, the EDS analyses revealed all the detected elemental components but yttria was not detected possibly due to its low content. Fairly enough, the distribution of the ceramic oxide was even and this gives the heterogeneous structure obtained in all the structures.

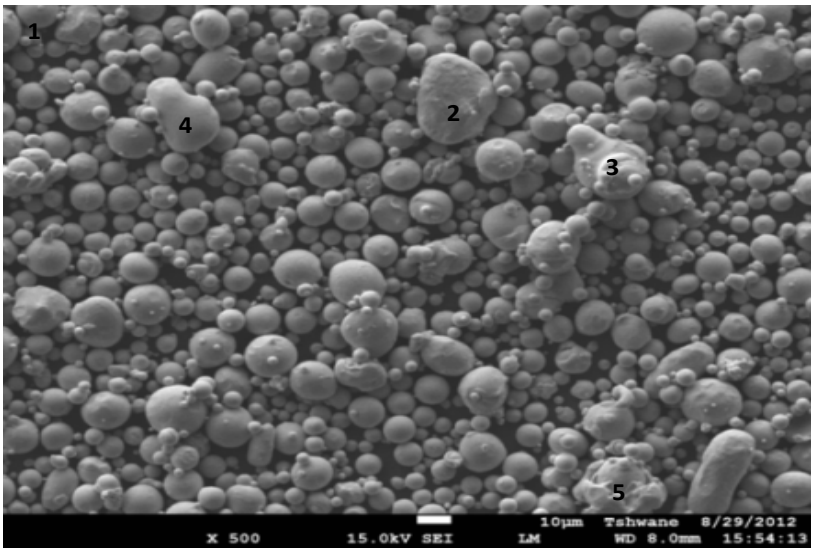

Figure 1. *SEM image of as-received 2205 DSS powder*

Table 3. EDS analyses of as-received 2205 DSS powder

Spectrum	C (%)	Si (%)	Cr (%)	Fe (%)	Ni (%)	Mo (%)	P (%)	Mn (%)	S (%)
1	7.58	0.67	23.96	59.93	4.09	3.74	-	-	-
2	-	1.16	23.70	66.02	4.65	3.74	0.73	-	-
3	-	1.22	24.02	68.10	5.11	-	-	-	1.52
4	2.59	0.85	-	63.37	5.04	3.89	-	1.42	-
5	5.50	0.99	22.86	61.95	4.84	3.83	-	-	-

The expected balance of austenitic and ferritic phases was observed in the sintered samples as shown in Figures 2. The light parts were the austenitic phase while the dark patches were the ferritic. Pores, identified by the black spots, were also observed. This is evident of PM. From the SEM micrographs, it was observed that introduction of alloying

elements help reduces the pore percentage present though; the pores continue to be on the rise with further addition of the ceramic oxide. This was balanced with further addition of the selected alloying elements which contain Ni, given that Ni has lower melting point, it was able to melt and flow in the matrix thereby filling up pores. There was also grain refinement by the ceramic oxide coupled with prevention of grain growth, the reinforcement ($ZrO_2(Y_2O_3)$) has different crystallographic orientations, as such, grain boundaries arises. During sintering, when pressure is applied, slip motion takes place. Grain boundaries then act as an impediment to pores movement [17].

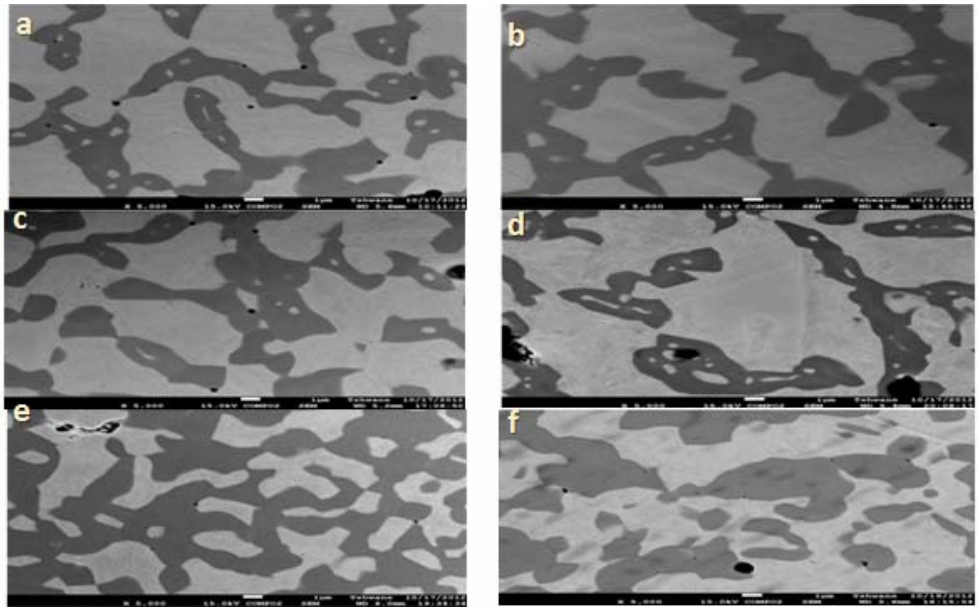

Figure 2. *SEM micrographs of sintered samples: (a) A1, (b) A2, (c) A3, (d) A4, (e) A5, (f) X*

Corrosion

The curves for ODS DSS 2205 (Figure 3) displayed similar behavior for all the MMC samples. There was initial shift in the more negative potential i.e. the active region for the first few seconds, after which there was slight shift back to the more positive region, an indication of passivation. The potential then stabilized, this was maintained for almost all the period of the experiment. However, sample A1 showed the most negative potential followed by sample X (sintered as-received) while sample A2 has the most positive potential. The indication of this was that sample A1 has the most corrosion susceptibility followed by the as-received 2205 (X). Other samples; A2, A3 and A4 are less corrosion susceptible than sintered as-received 2205 in simulated mine water. Sample A5 on the other hand, at the initial stage of the experiment showed higher potential but over time, shifted to a lower potential compared

with sample X. Addition of PSZ with Chromium and Nickel to 2205 DSS have influence on the polarization potential by shifting the potentials into the more positive region as can be observed for samples A1, A2 and A5 in Figure 3, however, for samples A3 and A4, the potentials were shifted in to the active region which indicated that corrosion susceptibility of samples A3 and A4 are higher than that of samples A1, A2 and A5. From the graphs, it was seen that sample A5 has the highest potential with the most shift in the positive potential.

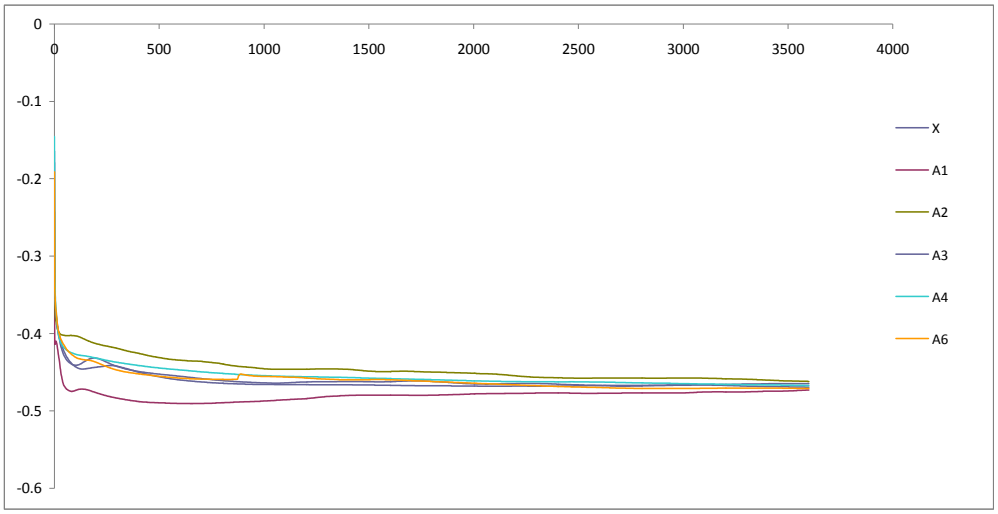

***Figure 3**. OCP measurement for 2205 DSS composites in simulated mine water*

Figure 4 is the potentiodynamic polarization results for 2205 DSS composites in simulated mine water. The polarization curves revealed the corrosion potential of each composite of 2205 and its composites. Taking composite X as the referential point; the potential of composite A1 was shifted in the more negative potential while A3 and A4 were slightly shifted in the more negative potential but A2 was almost the same with composite X. Possibility of this was that the incorporation of the dispersant (PSZ) has destabilize the balance of the original composition of the 2205 DSS in A1 and there was no further addition of Cr to affect positively the corrosion properties as shown in the corrosion current density. However, for composite samples A2, A3 and A4, though there were further incorporation of Cr and Ni, the Cr present might not be adequate to maintain the balance in the chemical composition or inhomogeneity in the composite or even combination of both as also revealed in the SEM images. For composite A5, the potential was shifted in the more positive potential. The implications of this was that A5 with the most positive potential has the least susceptibility to corrosion while sample A1 with the least potential has the highest

susceptibility to corrosion. Similar trend were observed from the corrosion current density which indicated that composite A5 has the least corrosion rate; A5 has the least corrosion rate as shown in Table 4. This could be connected to the percentage of Cr and Ni present in the composite matrix (2.4% Cr and 0.56% Ni).

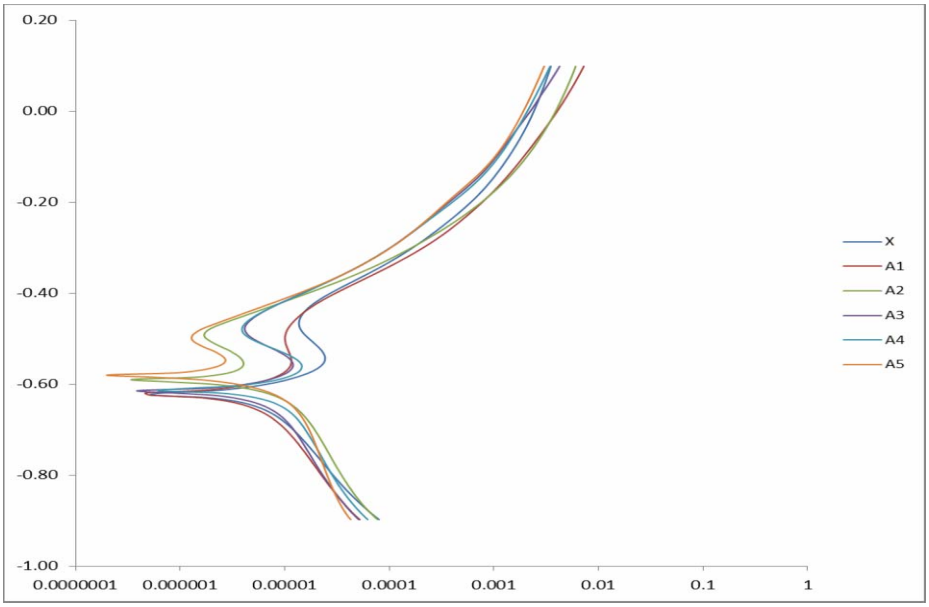

Figure 4. *Polarization curves of PM 2205 duplex stainless steel composite in simulated Mine water*

This clearly demonstrated that the Cr present in this composite is well enough to convert all the available carbon to carbide thereby suppressing the corrosion reaction rate as indicated from the current density shown from Figure 4. However, in sample A4, the Cr present is enough also to convert the carbon to carbide but the corrosion reaction might have been influenced by inhomogeneity due to high percentage of PSZ (3%). Also from the curves, there were region of passivation. However, there was no clear cut pitting potential revealed from the curves.

Table 4. Corrosion rate of 2205 DSS composites in simulated mine water

Sample	Ecorr	Icorr(A)	Icorr(A/cm^2)	bc(v/dec)	ba(v/dec)	Rp(Ω)	Cr(mm/yr)
X	-0.628	$5.82 \cdot 10^{-6}$	4.096E-6	0.116	0.229	1.972E3	4.844E-2
A1	-0.625	2.57E-6	2.545E-6	0.082	0.101	1.397E3	3.024E-2
A2	-0.595	1.70E-6	1.487E-6	0.086	0.035	7.573E2	1.769E-2
A3	-0.617	3.55E-6	2.793E-6	0.088	0.124	1.335E3	3.307E-2
A4	-0.619	6.05E-6	4.767E-6	0.138	0.161	1.586E3	5.657E-2
A5	-0.583	7.13E-7	5.612E-7	0.04	0.023	5.536E2	6.68E-3

From the potentio-dynamic polarization scan of 2205 composites in simulated mine

water, sample A5 has the highest corrosion potential (lowest corrosion susceptibility) which translated to lowest corrosion activity. This was revealed from the SEM image of the corrosion damaged surface of all the samples. Sample A5 showed the least damaged surface. This confirmed that Cr inclusion in sample A5 is enough for carbon conversion to carbide thereby leading to reduction of corrosion activity. Samples A3 and A4 had the most damaged surface of all the 2205 ODS DSS in simulated mine water. This indicated that Cr might not be enough, coupled with possibility of inhomogeneous of the powders during mixing as sample A4 can be said to have enough Chromium addition yet, it was affected [18].

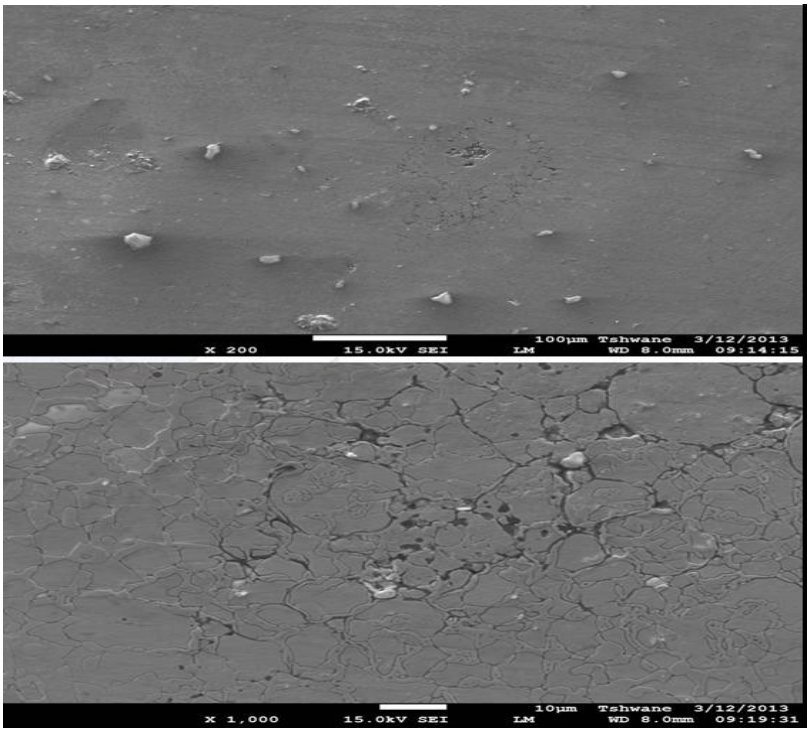

Figure 5. *Representation of SEM image of corroded sample in simulated mine water at different magnification.*

However, the attack of the simulated mine water on the ODS DSS composites was not that serious on the corrosion of the ODS DSS composites as revealed by the SEM images, (Figure 5); the surfaces were not severely damaged. This demonstrated that oxide dispersion strengthening with chromium addition with Nickel can enhance corrosion property of DSS composites.

Conclusions

Duplex stainless steel (2205) reinforced with different % composition of PSZ powders

were consolidated to full dense specimens by hot press sintering machine for 30min at 30MPa at the temperature 1100°C in argon gas environment. The final microstructures of the composites were found to be a function of the reinforcement and the alloying elements. Densification were further enhanced by the Ni addition which is characterized by a lower melting point and was able to melt and fill up the residual pores generated within the composite created by Zirconia and Chromium.

Acknowledgement

The authors wish to acknowledge the financial support received from Tshwane University of Technology (TUT), Pretoria, South Africa, National research Foundation (NRF) South Africa and the Federal University of Technology, Akure (FUTA). The authors thank R. Tabane and Meswi K. K. for the help in the experiments.

References

1. Olmos L., Martin C. L., Bouvard D., *Sintering of mixtures of powders: experiments and modelling*, Powder Technology, 2009, 190, p. 134-140.
2. Chen Z., Takeda T., Ikeda K., Murakami T., *The influence of powder particle size on microstructural evolution of metal-ceramic composite*, Scripta Matter, 2000, 43, p. 1103-1109.
3. Chaim R., Shlayer A., Estournes C., *Densification of nanocrystalline Y_2O_3 ceramic powder by spark plasma sintering*, J Eu Ceram Soc, 2009, 29, p. 91-98.
4. Karak S. K., Vishnu C. S., Witczak Z., Lojkowski W., Dutta M.J., Manna I., *Studies on wear behaviour of nano-Y_2O_3 dispersed ferritic steel developed by mechanical alloying and hot isostatic pressing*, Wear, 2010, 270, p. 5-11.
5. Reddy K. M., Mukhopadhyay A., Basu B., *Microstructure-mechanical-tribological property correlation of multistage spark plasma sintered tetragonal ZrO_2*, J Eur Cera Soc, 2010, 30, p. 3363-3375.
6. Youngmoo K., Kyong H. L., Eun-Pyo K., Dong_Ik C., Soon H. H., *Fabrication of high*

temperatures oxide dispersion strengthened tungsten composition by spark plasma sintering process, Int. J of Refractory Metals & Hard Materials, 2009, 27, p. 842-846.

7. Wong W. L. E., Gupta M., *Development of Mg/Cu nanocomposites using microwave assisted rapid sintering,* Composites Science and Technology, 2007, 67, p. 1541-1542.
8. Datta P., Upadhyaya G. S., *Sintered duplex stainless steels from premixes of 316L and 434L powders,* Materials Chemistry and Physics, 2001, 67, p. 234-242.
9. Glage A., Weigelt C., Rathel J., Biermann H., *Fatigue behavior of hot pressed austenitic TWIP steel and TWIP steel/Mg-PSZ composite materials,* International Journal of Fatigue, 2014, 65, p. 9-17.
10. Sebo P., Kavecky S., Stefanik P., *Wettability of Zirconia-coated carbon by aluminium*, J Mater Sci Letters, 1994, 13, p. 592-593.
11. Muolo M. L., Passerone V. A., Passerone D., *Oxygen influence on ceramics wettability by liquid metals Ag/α-Al_2O_3- Experiments and modelling*, Mater Sci and Eng: A, 2008, 3(495), p. 153-158.
12. Passerone A., Muolo M. L., Novakovic R., Passerone D., *Liquid matel/ceramic interactions in the (Cu, Ag, Au) / ZrB_2 systems*, J Eu Ceram Soc, 2007, 27, p. 3277-3285.
13. Wei D., Dave R., Pfeffer R., *Mixing and characterization of nanosized powders: An accessment of different techniques*, J Nanoparticle Research, 2002, 4, p. 21-41.
14. Chawla, N., Chawla, K. K., *Metal matrix composites,* New York: Springer, 2006.
15. Liu Y. B., Lim S. C., Lu L., Lai M. O., *Recent development in the fabrication of metal matrix-particulate composites using powder metallurgy techniques,* J Mater Sci, 1994, 29, p. 1999-2007.
16. Li W., Gao L., *Rapid sitering of nanochrystalline ZrO_2(3Y) by spark plasma sintering*. J Eu Ceram Soc, 2000, 20, p. 2441-2445.
17. Gang J., Thiery G., Nathali B., Sebastien L., *The mechanisms of microstructure formation in a nanostructured oxide dispersion strengthened FeAl alloy obtained by spark plasma sintering*, Intermetallics, 2007, 15, p. 108-118.
18. Olaniran O., Olubambi P. A., Potgieter B., Olaniran B., Adegbola A., Folorunso D., *Corrosion behaviour of PM ODS composite sintered in argon atmosphere*, Journal of Materials Science and Technology, 2013, 21(3), p. 186-193.